BULLETIN OF BIOMATHEMATICS

Bulletin of Biomathematics, 2023, 1(2), 124–152

https://bulletinbiomath.org
ISSN Online: 2980-1869 / Open Access
https://doi.org/10.59292/bulletinbiomath.2023007

RESEARCH PAPER

Transmission dynamics of an age-structured Hepatitis-B infection with differential infectivity

Umar Tasiu Mustapha [1,‡], **Yau Umar Ahmad** [1,‡], **Abdullahi Yusuf** [1,*,‡], **Sania Qureshi** [2,3,4,‡] **and Salihu Sabiu Musa** [5,6,‡]

[1]Department of Mathematics, Federal University Dutse, 7156 Jigawa, Nigeria, [2]Department of Basic Sciences and Related Studies, Mehran University of Engineering and Technology, Jamshoro 76062, Pakistan, [3]Department of Mathematics, Near East University, 99138 Mersin, Türkiye, [4]Department of Computer Science and Mathematics, Lebanese American University, Beirut, Lebanon, [5]Department of Applied Mathematics, Hong Kong Polytechnic University, Hong Kong SAR, China, [6]Department of Mathematics, Kano University of Science and Technology, Wudil, Nigeria

* Corresponding Author
‡ umar.tasiu@fud.edu.ng (Umar Tasiu Mustapha); yauumarahmad@gmail.com (Yau Umar Ahmad); yusufabdullahi@fud.edu.ng (Abdullahi Yusuf); sania.qureshi@faculty.muet.edu.pk (Sania Qureshi); salihu-sabiu.musa@connect.polyu.hk (Salihu Sabiu Musa)

Abstract

An age-structured deterministic mathematical model describing the transmission dynamics of Hepatitis B (HBV) is proposed in this paper. The model exhibits the phenomenon of backward bifurcation in which a stable disease-free equilibrium coexists with a stable endemic equilibrium as the basic reproduction number (BRN) approaches one. The epidemiological consequence of backward bifurcation is that the requirement for making the BRN less than one is necessary but not sufficient condition for efficiently controlling the persistence of the disease in the human population. We estimate the model parameters with the help of real data from South Africa using the nonlinear least-squares curve fitting method. We also use the forward normalized sensitivity index technique to determine the most sensitive parameters. Numerical simulations confirm that reducing the transition of chronically infected children to adults through treatment is crucial to eliminating Hepatitis-B in South Africa.

Keywords: Hepatitis-B; age-structured model; parameter estimation; bifurcation; sensitivity analysis
AMS 2020 Classification: 34C23; 62P10; 92B05; 92D25

1 Introduction

Hepatitis refers to liver inflammation caused by a virus. Five different strains of virus cause hepatitis; hepatitis type A, B, C, D, and E written as HAV, HBV, HCV, HDV, and HEV, respectively.

➤ **Received:** 21.08.2023 ➤ **Revised:** 25.10.2023 ➤ **Accepted:** 28.10.2023 ➤ **Published:** 30.10.2023

Viral hepatitis is a life-threatening disease that caused 1.34 million deaths, which is a number comparable to the annual mortality caused by tuberculosis and greater than that of HIV in 2015 [1]. Over the years (30 or more), plans to eradicate viral hepatitis have increased through different public health activities. The World Health Assembly first recommended the HBV vaccine into routine infant immunization in the 1990s to reduce perinatal and early childhood transmission [1]. The vaccine control strategy was then improved in the 2000s with strategies on blood safety, healthcare injection safety, injection control, and minimizing the number of people who self-inject drugs [1]. These combined strategies reduced the perinatal and early childhood transmission, however, people progressing into chronic are still not minimized because of the lack of access (due to people who do not know their status and the medications are very expensive) to HBV and HCV treatment.

HBV is the most common infectious, and endemic among the five strains. Hepatitis B is a viral disease that attacks the liver causing it not to perform its usual functions (such as; processing of nutrients, filtration of blood, and fighting infections). The disease has an incubation period of two to three months and its symptoms include yellowing of skin and eye, weight loss, loss of appetite, dark urine, pale stool, fatigue, and abdominal pain [2]. HBV has an acute and chronic stage. Acute HBV disease lasts not longer than six months and the patient may freely recover from the disease, in fact, it is true for 4 in 5 adults who are infected [2]. Contrarily, if an infected person is living with the disease for a time greater than six months such person is said to be infected with the chronic HBV. Acute and chronically infected individuals may and may not have symptoms [2]. Acute and chronic infected individuals are both infectious but chronic infected individuals spread the disease more than the acute ones. The infectiousness also differs between the children and adults with more among the children than the adult. The chance of developing chronic HBV is higher among children than adults, 95% of the acute infants infected from their mothers or before the age of 5 years developed chronic HBV and only 5% among adults [2]. HBV can be transmitted vertically during the childbirth. This transmission does not imply that HBV is genetic, it is also called perinatal transmission.

The disease can also be transmitted horizontally via sexual transmission with the infected persons or exposure to infected blood (through reckless unscreened blood transfusion, unsafe injection, or exposure to sharp instrument that carries infected blood as the virus lives for seven days outside) [3]. Chronic HBV can be treated with medicines, including oral antiviral agents like Livolin, Lamivudine, Adefovir, etc. These drugs protect liver cells from viral damage, protect against progression into liver cancer, and reduce mortality due to HBV. However, access to HBV treatment is limited due to the lack of HBsAg and HBeAg tests. As of 2019, only 30.4 million people which is equivalent to 10.5% of the 296 million people estimated to be living with HBV are aware of their infections, while only 6.6 million people (22%) of the people diagnosed were on treatment [2].

40% of the world's total population had contact with HBV infection. Geographically HBV prevalence differs between the WHO regions, also the mode of transmission differs from one region to another. Transmission in high prevalence areas is predominantly mother-child, mostly during childbirth. This area has a prevalence of 10%-20% and the states under this category include; South Asia, China, and Sub-Saharan Africa. Intermediate prevalence transmission is mostly horizontal during childhood. The intermediate prevalence area has 3%-5% HBV infection prevalence and the countries include; Mediterranean countries, Japan, central Asia, the Middle East, and Latin and South America. Lower prevalence transmission is predominantly via sexual intercourse. The lower region has 0.1%-2% prevalence and the countries are Western Europe, the United States, Canada, Australia, and New Zealand [1, 4]. Research in 2015 showed that 257 million people were living with chronic HBV and about 1 million death cases yearly [1].

Further research in 2019 showed that 296 million people were living with chronic HBV and the

disease led to the death of 820,000 people [2]. HBV was highly endemic in South Africa (9.6% prevalence of chronic carriage in black South Africans and 76% exposed to HBV) before the introduction of vaccine (HepB3) in 1995 [5, 6]. HBV transmission is mostly horizontal in South Africa, especially between children less than 5 years of age. The disease prevalence among children 5 years of age declined from 12.8% before the vaccine was introduced to 3.0% in 2009 [5]. Between the period of 2000 to 2018, HepB3 coverage in South Africa averaged 76.6%.

The idea of a compartmental model first appeared in the 1920s [7]. The epidemic models Kermack-McKendrick (1927) and Reed-Frost (1928) both depict the interaction between susceptible, infected, and immune individuals in a community [8]. Since then, researchers have studied disease with an SIR model to predict the transmission dynamics and the possibility of controlling the disease by applying control strategies. This leads to the recent studies on the analysis and local bifurcation of the SIR model or prey-predator model such as [9–11]. Mathematical modeling of disease is continuously in existence, the recent coronavirus disease pandemic attracted a lot of researchers to write thousands of papers on the transmission dynamics of the disease among are [12–15].

Many mathematical models have been proposed in the literature to study HBV dynamics. Age is one of the significant characteristics in mathematical epidemiology [16]. Few researchers developed age-structured mathematical models in studying Hepatitis B among are [17–24]. The current paper describes HBV model analysis with vital dynamics and heterogeneous mixture. The details transition flow with differential infectivity is the most important aspect of this study and therefore future researchers especially those interested in optimal control analysis can use the model to determine the best among available control strategies. Finding the best control strategy will directly help policymakers like WHO in controlling the HBV disease as the target year (2030) of elimination is fast approaching.

The paper is organized as follows: Section 2 contains model formulation, Section 3 contains model analysis, Section 4 involves model fitting and parameters estimations, sensitivity analysis is carried out in Section 5, while Section 6 and Section 7 contain numerical simulations, discussion, and conclusion respectively.

2 Model formulation

The model is developed to study the transmission dynamics of Hepatitis B viral infection. The total population denoted by $N(t)$ is divided into seven disjoint compartments. Susceptible children $S_c(t)$, susceptible adult $S_a(t)$, children infected with acute HBV $A_c(t)$, children infected with chronic HBV $C_c(t)$, adult infected with acute HBV $A_a(t)$, adult infected with chronic HBV $C_a(t)$ and the removed or recovered compartment $R(t)$. The recruitment into the susceptible class is by birth and migration at a constant rate π. Progression from susceptible children into susceptible adult ϕ compartment is by age. The susceptible population decreases with the emergence of the infection at the rate λ. Children are more susceptible to becoming infected (this is the reason for adding the parameter θ reducing the rate of infection in adults). The probability of being infected with the disease is higher when in contact with a chronic infectious individual (α_1 and α_2 are used as parameters increasing the transmission rate by chronic individuals). The proportion of acutely infected children who progress into chronic is greater than that of adult (i.e. $q > k$). Progression from chronically infected children compartment into chronically infected adult compartment τ is by age. The mortality rate δ due to disease only occurs in the chronic infection compartment (so we consider any death in the acute infection compartment as natural death μ). The transmission rate which is the force of infection is given by;

$$\lambda = \frac{\beta(A_a + A_c + \alpha_1 C_c + \alpha_2 C_a)}{N},$$

where β is the contact rate and,

$$N(t) = S_c(t) + S_a(t) + A_c(t) + A_a(t) + C_c(t) + C_a(t) + R(t).$$

Figure 1 gives the schematic diagram of the model with the model equations given in system (1).

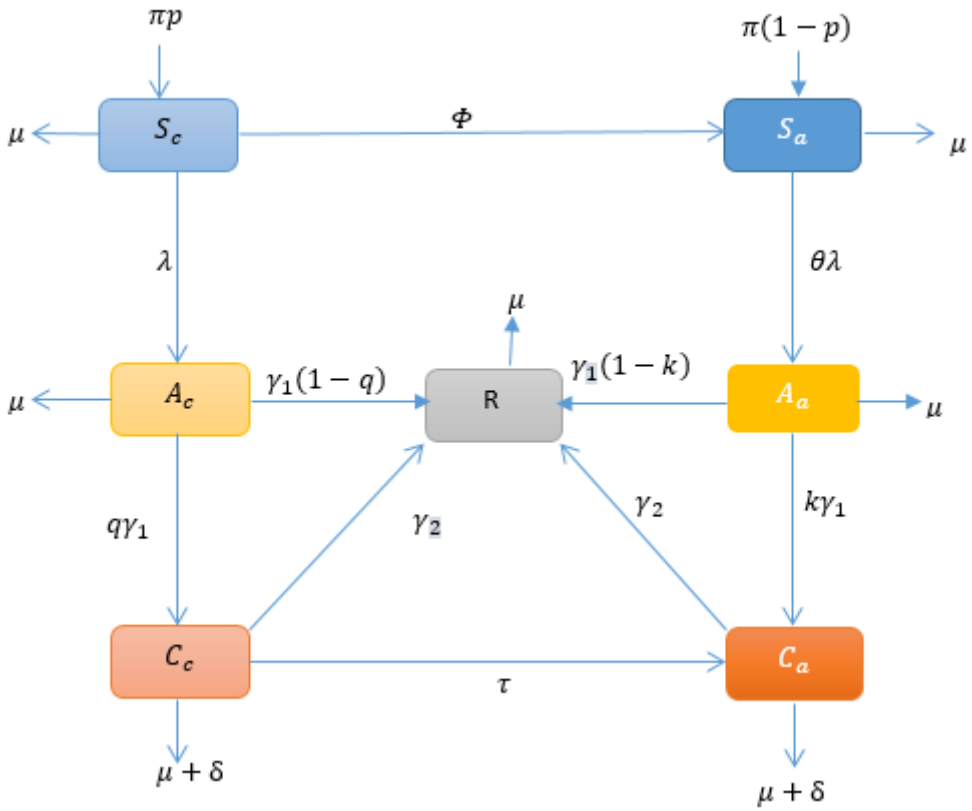

Figure 1. Schematic diagram of model (1). Solid arrows indicate transitions and expressions next to arrows show the *per capita* flow rate between compartments.

By taking into the given information above and the schematic diagram, the system of the disease can be written as:

$$\begin{aligned}
\frac{dS_c}{dt} &= \pi p - \phi S_c - \lambda S_c - \mu S_c,\\
\frac{dS_a}{dt} &= \pi(1-p) + \phi S_c - \theta\lambda S_a - \mu S_a,\\
\frac{dA_c}{dt} &= \lambda S_c - (\gamma_1 + \mu)A_c,\\
\frac{dA_a}{dt} &= \theta\lambda S_a - (\gamma_1 + \mu)A_a,\\
\frac{dC_c}{dt} &= q\gamma_1 A_c - (\gamma_2 + \tau + \mu + \delta)C_c,\\
\frac{dC_a}{dt} &= k\gamma_1 A_a + \tau C_c - (\gamma_2 + \mu + \delta)C_a,\\
\frac{dR}{dt} &= \gamma_1[(1-q)A_c + (1-k)A_a] + \gamma_2(C_c + C_a) - \mu R.
\end{aligned} \tag{1}$$

The variables and parameters with their interpretations are summarized in Table 1.

Table 1. Description of the variables and parameters used in the model (1).

Variable	Description
N	Total human population
S_c	Susceptible children
S_a	Susceptible adult
A_c	Acute infected children
A_a	Acute infected adult
C_c	Chronic infected children
C_a	Chronic infected adult
R	Recovered individuals
Parameter	**Description**
π	Recruitment rate
p	Fraction of π that is a child
μ	Natural death rate
ϕ	Progression rate from susceptible children into susceptible adult
β	Contact rate
α_1, α_2	Modification parameter increasing the infectiousness of chronically infected children and adults, respectively
θ	Modification parameter decreasing the chance of becoming infected of susceptible adult
τ	Progression rate of chronically infected children that grow into adult
q	Fraction of acutely infected children that becomes chronic
k	Fraction of acutely infected adult that becomes chronic
γ_1	Rate of leaving acute class
γ_2	Rate of leaving chronic infection class
δ	Disease-induced death rate

3 Basic properties of the model

Boundedness and positivity of solutions

Theorem 1 *The closed set*

$$D = \left\{ (S_c(t), S_a(t), A_c(t), A_a(t), C_c(t), C_a(t), R(t)) \, \epsilon \, R_+^7 : N \leq \frac{\pi}{\mu} \right\},$$

is positively invariant and attracts all positive solutions of the model. We have a single species of human population and so they can be in the same invariant set.

Proof We are to show that R_+^7 is positively invariant, that is all solutions of system (1) initiated in D do not leave D. Now, from the third, fourth, fifth, sixth, and seventh equation of (1), we obtain that,

$$\begin{aligned}
\frac{dA_c(t)}{dt} &\geq -(\gamma_1 + \mu)A_c, \quad \text{for} \;\; t \in [0, \tilde{t}), \\
\frac{dA_a(t)}{dt} &\geq -(\gamma_1 + \mu)A_a, \quad \text{for} \;\; t \in [0, \tilde{t}), \\
\frac{dC_c(t)}{dt} &\geq -(\gamma_2 + \tau + \mu + \delta)C_c, \quad \text{for} \;\; t \in [0, \tilde{t}), \\
\frac{dC_a(t)}{dt} &\geq -(\gamma_2 + \mu + \delta)C_a, \quad \text{for} \;\; t \in [0, \tilde{t}).
\end{aligned} \tag{2}$$

Now, let $S_c(0) > 0, S_a(0) > 0, A_c(0) > 0, A_a(0) > 0, C_c(0) > 0, C_a(0) > 0$, and $R(0)) > 0$. Suppose $S_c(0)$ and $S_a(0)$ are non-positive, then there exists a time $\tilde{t} > 0$, such that $S_c(t) > 0$ and $S_a(t) > 0$ for $t \in [0, \tilde{t})$ and $S_c(\tilde{t}) = S_a(\tilde{t}) = 0$. It follows that $A_c(0) > 0, A_a(0) > 0, C_c(0) > 0$ and $C_a(0) > 0$ for $t \in [0, \tilde{t})$. Thus, from the first and second equations of system (1), we have

$$\begin{aligned} \frac{dS_c(t)}{dt} &\geq -(\phi + \lambda + \mu)S_c(t), \quad \text{for } t \in [0, \tilde{t}), \\ \frac{dS_a(t)}{dt} &\geq -(\theta\lambda + \mu)S_a(t), \quad \text{for } t \in [0, \tilde{t}). \end{aligned}$$

One can clearly see that, $S_c(0) > 0$ and $S_a(0) > 0$ which contradict our assumption of $S_c(\tilde{t}) = S_a(\tilde{t}) = 0$. Hence $S_c(t)$ and $S_a(t)$ are positive. Similarly, positivity of subsystem (1) excluding the first and second equation can be written in matrix form as follows,

$$\frac{dX(t)}{dt} = \mathcal{A}Y(t) + B(t), \tag{3}$$

with,

$$\begin{aligned} X(t) &= \begin{pmatrix} A_c & A_a & C_c & C_a & R \end{pmatrix}^T, \\ \mathcal{A} &= \begin{pmatrix} K_1 - D_1 & K_1 & \alpha_1 K_1 & \alpha_2 K_1 & 0 \\ K_2 & K_2 - D_1 & \alpha_1 k_2 & \alpha_2 k_2 & 0 \\ q\gamma_1 & 0 & -D_2 & 0 & 0 \\ 0 & k\gamma_1 & \tau & -D_3 & 0 \\ \gamma_1(1-q) & \gamma_1(1-k) & \gamma_2 & \gamma_2 & -\mu \end{pmatrix}, \\ B(t) &= \begin{pmatrix} 0 & 0 & 0 & 0 & 0 \end{pmatrix}^T, \end{aligned} \tag{4}$$

where, $K_1 = \frac{\beta S_c^0}{N}, K_2 = \frac{\beta\theta S_a^0}{N}, D_1 = \gamma_1 + \mu, D_2 = \gamma_2 + \tau + \mu + \delta$ and $D_3 = \gamma_2 + \mu + \delta$.

Clearly, $\mathcal{A}$ is a Metzler (upper diagonal matrix is positive) matrix for the fact that both $S_c(t)$ and $S_a(t)$ are non-negative, which shows subsystem (3) is a monotone system. As such, $\mathbb{R}^5_+$ is invariant under the flow of subsystem (3). Hence, D is positively invariant and attract all the positive solution of system (1). ■

Disease-free equilibrium point

To determine the disease-free equilibrium (DFE) point, we set the right-hand sides of system (1) to zero and considered all the infection variables equal to zero, then we derived the DFE point (ϵ^0) of the model as

$$\epsilon^0 = (S_c^0, S_a^0, A_c^0, A_a^0, C_c^0, C_a^0, R^0) = \left(\frac{\pi p}{\phi + \mu}, \frac{\pi(\phi + \mu - \mu p)}{\mu(\phi + \mu)}, 0, 0, 0, 0, 0\right).$$

It implies that at the disease-free equilibrium, the total population $N(t)$ is,

$$N^0 = \frac{\pi}{\mu}.$$

Basic reproduction number

The basic reproduction number denoted by R_0 refers to the average number of secondary infections that occur when a single carrier is introduced into a completely susceptible host population. The basic reproduction number is used for the stability analysis of system (1). The next generation matrix technique as described by [25], is used to obtain the basic reproduction number which is given by $R_0 = \rho(FV^{-1})$, where ρ is the spectral radius or the dominant eigenvalue of the next generation matrix FV^{-1}, as follows:

The matrices F (for the new infection terms) and V (for the remaining transition terms) associated with model (1) are respectively given by:

$$F = \begin{bmatrix} \frac{\beta S_c^0}{N^0} & \frac{\beta S_c^0}{N^0} & \frac{\alpha_1 \beta S_c^0}{N^0} & \frac{\alpha_2 \beta S_c^0}{N^0} \\ \frac{\beta\, \theta S_a^0}{N^0} & \frac{\beta\, \theta S_a^0}{N^0} & \frac{\alpha_1 \beta\, \theta S_a^0}{N^0} & \frac{\alpha_2 \beta\, \theta S_a^0}{N^0} \\ 0 & 0 & 0 & 0 \\ 0 & 0 & 0 & 0 \end{bmatrix}, \tag{5}$$

$$V = \begin{bmatrix} D_1 & 0 & 0 & 0 \\ 0 & D_1 & 0 & 0 \\ -q\gamma_1 & 0 & D_2 & 0 \\ 0 & -k\gamma_1 & -\tau & D_3 \end{bmatrix}, \tag{6}$$

the inverse matrix of V is given as

$$V^{-1} = \begin{bmatrix} \frac{1}{D_1} & 0 & 0 & 0 \\ 0 & \frac{1}{D_1} & 0 & 0 \\ \frac{q\gamma_1}{D_1 D_2} & 0 & \frac{1}{D_2} & 0 \\ \frac{\tau q \gamma_1}{D_1 D_2 D_3} & \frac{k\gamma_1}{D_1 D_3} & \frac{\tau}{D_2 D_3} & \frac{1}{D_3} \end{bmatrix}, \tag{7}$$

$$FV^{-1} = \begin{bmatrix} \frac{\beta S_c^0}{N^0 D_1} + \frac{\alpha_1 \beta S_c^0 q\gamma_1}{N^0 D_2 D_1} + \frac{\alpha_2 \beta S_c^0 \tau\, q\gamma_1}{N^0 D_2 D_1 D_3} & \frac{\beta S_c^0}{N^0 D_1} + \frac{\alpha_2 \beta S_c^0 k\gamma_1}{N^0 D_1 D_3} & \frac{\alpha_1 \beta S_c^0}{N^0 D_2} + \frac{\alpha_2 \beta S_c^0 \tau}{N^0 D_2 D_3} & \frac{\alpha_2 \beta S_c^0}{N^0 D_3} \\ \frac{\beta\, \theta S_a^0}{N^0 D_1} + \frac{\alpha_1 \beta\, \theta S_a^0 q\gamma_1}{N^0 D_2 D_1} + \frac{\alpha_2 \beta\, \theta S_a^0 \tau\, q\gamma_1}{N^0 D_2 D_1 D_3} & \frac{\beta\, \theta S_a^0}{N^0 D_1} + \frac{\alpha_2 \beta\, \theta S_a^0 k\gamma_1}{N^0 D_1 D_3} & \frac{\alpha_1 \beta\, \theta S_a^0}{N^0 D_2} + \frac{\alpha_2 \beta\, \theta S_a^0 \tau}{N^0 D_2 D_3} & \frac{\alpha_2 \beta\, \theta S_a^0}{N^0 D_3} \\ 0 & 0 & 0 & 0 \\ 0 & 0 & 0 & 0 \end{bmatrix}. \tag{8}$$

We therefore obtain the basic reproduction number R_0 by substituting S_c^0, S_a^0 and N^0 as

$$R_0 = \frac{\beta\ (\phi + \mu - \mu p)(k\theta\alpha_2 D_2\gamma_1 + \theta D_2 D_3) + \beta\mu p(\tau q\alpha_2\gamma_1 + q\alpha_1 D_3\gamma_1 + D_2 D_3)}{D_1 D_2 D_3(\phi + \mu)}, \tag{9}$$

where $D_1 = \gamma_1 + \mu, D_2 = \gamma_2 + \tau + \mu + \delta$ and $D_3 = \gamma_2 + \mu + \delta$.

R_0 here is interpreted as the number of secondary infections produced by children with acute HBV infection, adults with acute HBV infection, children with chronic HBV infection, and adults with chronic HBV infection when a single acute or chronic infected individual introduced in the absence of any control measure.

Local stability of the DFE

Theorem 2 *Assume that no acutely infected individual developed chronic Hepatitis B ($k = q = 0$), then the disease-free equilibrium, E^0, of the model (1) is locally-asymptotically stable in D if $R_0 < 1$, and unstable if $R_0 > 1$.*

Proof We linearize the system by taking the Jacobian matrix of system (1) at the DFE as explained in the Subsection 3,

$$J(\epsilon^0) = \begin{bmatrix} -\phi-\mu & 0 & -\beta K_1 & -\beta K_1 & -\beta\alpha_1 K_1 & -\beta\alpha_2 K_1 & 0 \\ \phi & -\mu & -\beta\theta K_2 & -\beta\theta K_2 & -\beta\theta\alpha_1 K_2 & -\beta\theta\alpha_2 K_2 & 0 \\ 0 & 0 & \beta K_1 - D_1 & \beta K_1 & \beta\alpha_1 K_1 & \beta\alpha_2 K_1 & 0 \\ 0 & 0 & \beta\theta K_2 & \beta\theta K_2 - D_1 & \theta\alpha_1 K_2 & \theta\alpha_2 K_2 & 0 \\ 0 & 0 & q\gamma_1 & 0 & -D_2 & 0 & 0 \\ 0 & 0 & 0 & k\gamma_1 & \tau & -D_3 & 0 \\ 0 & 0 & \gamma_1(1-q) & \gamma_1(1-k) & \gamma_2 & \gamma_2 & -\mu \end{bmatrix}, \tag{10}$$

where $K_1 = \frac{\mu p}{\phi+\mu}, K_2 = \frac{\phi+\mu(1-p)}{\phi+\mu}$, reducing Eq. (10) into row-echelon form gives Eq. (11) below,

$$J(\epsilon^0) = \begin{bmatrix} a_{11} & 0 & a_{13} & a_{14} & a_{15} & a_{16} & 0 \\ 0 & a_{22} & a_{23} & a_{24} & a_{25} & a_{26} & 0 \\ 0 & 0 & a_{33} & a_{34} & a_{35} & a_{36} & 0 \\ 0 & 0 & 0 & a_{44} & a_{45} & a_{46} & 0 \\ 0 & 0 & 0 & 0 & a_{55} & a_{56} & 0 \\ 0 & 0 & 0 & 0 & 0 & a_{66} & 0 \\ 0 & 0 & 0 & 0 & 0 & 0 & a_{77} \end{bmatrix}, \tag{11}$$

where

$$\begin{aligned} a_{11} = -(\phi+\mu), a_{13} = -\beta K_1, a_{14} = -\beta K_1, a_{15} = -\beta\alpha_1 K_1, a_{16} = -\beta\alpha_2 K_2, a_{22} = -\mu(\phi+\mu), \\ a_{23} = -\beta\phi K_1 - \beta\theta k_2(\phi+\mu), a_{24} = -\beta\phi K_1 - \beta\theta K_2(\phi+\mu), a_{25} = -\beta\phi\alpha_1 K_1 - \beta\theta\alpha_1 K_2(\phi+\mu), \\ a_{26} = -\beta\phi\alpha_2 K_1 - \beta\theta\alpha_2 K_2(\phi+\mu), a_{33} = \beta K_1 - D_1, a_{34} = \beta K_1, a_{35} = \beta\alpha_1 K_1, a_{36} = \beta\alpha_2 K_1, \\ a_{44} = \beta^2\theta K_1 K_2 - (\beta K_1 - D_1)(\beta\theta K_2 - D_1), a_{45} = \beta^2\theta\alpha_1 K_1 K_2 - (\beta K_1 - D_1)(\theta\alpha_1 K_2), \\ a_{46} = \beta^2\theta\alpha_2 K_1 K_2 - (\beta K_1 - D_1)(\theta\alpha_2 K_2), a_{55} = \beta\gamma_1 q K_1 a_{45} - a_{44}[\beta\gamma_1\alpha_1 q K_1 + D_2(\beta K_1 - D_1)], \\ a_{56} = \beta\gamma_1 q K_1 a_{46} - \beta\gamma_1\alpha_2 q K_1 a_{44}, a_{66} = a_{56}(k\gamma_1 a_{45} - \tau a_{44}) - a_{55}(k\gamma_1 a_{46} - D_3 a_{44}), \\ a_{77} = -\mu a_{33} a_{44} a_{55} a_{66}, \end{aligned} \tag{12}$$

and the eigenvalues are,

$$\begin{bmatrix} \lambda_1 = a_{77} \\ \lambda_2 = a_{66} \\ \lambda_3 = a_{55} \\ \lambda_4 = a_{44} \\ \lambda_5 = a_{33} \\ \lambda_6 = a_{22} \\ \lambda_7 = a_{11} \end{bmatrix}, \tag{13}$$

clearly, $\lambda_7 = a_{11}$ and $\lambda_6 = a_{22}$ are negative from Eq. (12). And for the other eigenvalues, we have,

$$a_{33} = \beta K_1 - D_1, \tag{14}$$

substitute for K_1,

$$\Rightarrow \frac{\beta\mu p}{\phi + \mu} - D_1 < 0,$$

$$\iff \frac{\beta\mu p}{D_1(\phi + \mu)} < 1, \tag{15}$$

so $\lambda_5 = a_{33}$ is negative if and only if Eq. (15) holds.

$$a_{44} = \beta^2\theta K_1 K_2 - (\beta K_1 - D_1)(\beta\theta K_2 - D_1), \tag{16}$$

$$\beta K_1 D_1 + \beta\theta K_2 D_1 - D_1^2 < 0,$$

$$\iff \frac{\beta K_1}{D_1} + \frac{\beta\theta K_2}{D_1} < 1,$$

$$\frac{\beta\mu p}{D_1(\phi + \mu)} + \frac{\beta\theta(\phi + \mu(1-p))}{D_1(\phi + \mu)} < 1, \tag{17}$$

so, $\lambda_4 = a_{44} < 0$ if and only if Eq. (17) is satisfied.

$$\begin{aligned} a_{55} &= -a_{33}a_{44}D_2, \\ a_{66} &= -a_{44}a_{55}D_3, \\ a_{77} &= -\mu a_{33}a_{44}a_{55}a_{66}, \end{aligned}$$

clearly, $\lambda_3 = a_{55} < 0$, $\lambda_2 = a_{66} < 0$, $\lambda_1 = a_{77} < 0$, substituting $k = q = 0$ in the calculated basic

reproduction number R_0 of (9), the basic reproduction number reduced to

$$R_0 = \frac{\beta\mu p}{D_1(\phi+\mu)} + \frac{\beta\theta(\phi+\mu(1-p))}{D_1(\phi+\mu)}, \tag{18}$$

observed that Eqs. (17) and (18) are the same. Therefore, all the eigenvalues are negative, $\lambda_i < 0$ for all i whenever $R_0 < 1$. Hence applying the Routh-Hurwitz criterion as in [26, 27], the disease-free equilibrium is locally asymptotically stable when $R_0 < 1$. ■

Global stability of the DFE

Theorem 3 *The disease-free equilibrium (DFE) ϵ^0, of model (1), is globally-asymptotically stable (GAS) in D if $R_0 < 1$ and unstable if $R_0 > 1$.*

Proof To prove the theorem above, two conditions (H1) and (H2) as in [28] must be satisfied for $R_0 < 1$. The model can be written in the form;

$$\begin{aligned} \frac{dX_1}{dt} &= F(X_1, X_2), \\ \frac{dX_2}{dt} &= G(X_1, X_2); G(X_1, 0) = 0, \end{aligned} \tag{19}$$

where $X_1 = (S_c^0, S_a^0, R^0)$ and $X_2 = (A_c^0, A_a^0, C_c^0, C_a^0)$. Here $X_1 \in R_+^3$ denotes the uninfected population and $X_2 \in R_+^4$ denoting the infected population. The disease-free equilibrium is now denoted as, $E^0 = (X_1^*, 0)$, where $X_1^* = (N^0, 0)$. Now for the first condition, global asymptotic stability of X_1^*, gives

$$\frac{dX_1}{dt} = F(X_1, 0) = \begin{bmatrix} \pi p - (\phi+\mu)S_c^0 \\ \pi(1-p) + \phi S_c^0 - \mu S_a^0 \\ -\mu R^0 \end{bmatrix}. \tag{20}$$

Solving the ODE gives,

$$\begin{aligned} \frac{\pi p}{(\phi+\mu)} - \frac{\pi p}{(\phi+\mu)} e^{-(\phi+\mu)t} + S_c^0(0)e^{-(\phi+\mu)t} &= S_c^0(t), \\ \frac{\pi(1-p)+\phi S_c^0}{\mu} - \frac{\pi(1-p)+\phi S_c^0}{\mu} e^{-\mu t} + S_a^0(0)e^{-\mu t} &= S_a^0(t), \\ R^0(t)e^{-\mu t} &= R^0(t). \end{aligned}$$

Now, clearly from system (1), we have, $S_c^0(t) + S_a^0(t) + R^0(t) \to N^0(t)$ as $t \to \infty$ regardless of the value of $S_c^0(t), S_a^0(t)$ and $R^0(t)$. Thus, $X_1^* = (N^0, 0)$ is globally asymptotically stable.
Next, for the second condition, that is $\tilde{G}(X_1, X_2) = AX_2 - G(X_1, X_2) \geq 0$,

$$A = \begin{pmatrix} -(\gamma_1+\mu) + \frac{\beta}{N} & \frac{\beta}{N} & \frac{\beta\alpha_1}{N} & \frac{\beta\alpha_1}{N} \\ \frac{\beta\theta}{N} & \frac{\beta\theta}{N} - (\gamma_1+\mu) & \frac{\beta\theta\alpha_1}{N} & \frac{\beta\theta\alpha_2}{N} \\ q\gamma_1 & 0 & -(\gamma_2+\tau+\mu+\delta) & 0 \\ 0 & k\gamma_1 & \tau & -(\gamma_2+\mu+\delta) \end{pmatrix}. \tag{21}$$

Matrix A is a Metziller matrix (the off-diagonal elements are non-negative).

$$G(X_1, X_2) = \begin{pmatrix} \frac{\beta(A_a^0 + A_c^0 + \alpha_1 C_c^0 + \alpha_2 C_a^0)}{N^0} S_c^0 - (\gamma_1 + \mu) A_c^0 \\ \frac{\theta\beta(A_a^0 + A_c^0 + \alpha_1 C_c^0 + \alpha_2 C_a^0)}{N^0} S_a^0 - (\gamma_1 + \mu) A_a^0 \\ q\gamma_1 A_c^0 - (\gamma_2 + \tau + \mu + \delta) C_c^0 \\ k\gamma_1 A_a^0 + \tau C_c^0 - (\gamma_2 + \mu + \delta) C_a^0 \end{pmatrix}. \tag{22}$$

Then,

$$\tilde{G}(X_1, X_2) = AX_2 - G(X_1, X_2) = \begin{bmatrix} 0 \\ 0 \\ 0 \\ 0 \end{bmatrix}.$$

That is,

$$\tilde{G}(X_1, X_2) = \begin{bmatrix} 0 & 0 & 0 & 0 \end{bmatrix}^T.$$

It is obvious that $\tilde{G}(X_1, X_2) = 0$. ■

Endemic equilibrium point

As HVB enters into the population at least one of the infection classes is not empty. Finding the explicit solution of equilibrium points in a model with a recruitment rate not equal to the death rate in terms of the parameters of the model is tedious and sometimes inconvenient. As such, equating the vector field of Eq. (1) to zero, the endemic equilibrium points in terms of the force of infection are determined after algebraic manipulations. The set of endemic equilibrium point is given by:

$$\epsilon^* = (S_c^*, S_a^*, A_c^*, A_a^*, C_c^*, C_a^*),$$

where

$$\begin{aligned}
S_c^* &= \frac{\pi\, p}{\lambda^* + \mu + \phi}, \\
S_a^* &= -\frac{\pi\, ((p-1)\lambda^* + (p-1)\mu - \phi)}{(\lambda^* \theta + \mu)(\lambda^* + \mu + \phi)}, \\
A_c^* &= \frac{\lambda^* \pi\, p}{(\lambda^* + \mu + \phi) D_1}, \\
A_a^* &= -\frac{\lambda^* \theta\, \pi\, ((p-1)\lambda^* + (p-1)\mu - \phi)}{D_1 (\lambda^* \theta + \mu)(\lambda^* + \mu + \phi)}, \\
C_c^* &= \frac{q\lambda^* \pi\, p\gamma_1}{D_1 D_2 (\lambda^* + \mu + \phi)}, \\
C_a^* &= -\frac{\gamma_1 \lambda^* \pi\, ((((p-1)\lambda^* + (p-1)\mu - \phi) kD_2 - \lambda^* pq\tau)\theta - \mu\, pq\tau)}{D_3 D_2 D_1 (\lambda^* \theta + \mu)(\lambda^* + \mu + \phi)}.
\end{aligned} \tag{23}$$

Existence of the endemic equilibrium

Descartes' rule of sign is used in concluding the existence. Now at endemic states, the force of infection is given by,

$$\lambda^* = \frac{\beta(A_c^* + A_a^* + \alpha_1 C_c^* + \alpha_2 C_a^*)}{N^*},$$

where,

$$N^* = S_c^* + S_a^* + A_c^* + A_a^* + C_c^* + C_a^*,$$

substituting for the endemic equilibrium points into the force of infection above gives $\lambda^* = 0$. equivalent to DFE which is stable, and the following quadratic equation in terms of λ^*,

$$A{\lambda^*}^2 + B\lambda^* + C = 0,$$

where,

$$\begin{aligned}
A =& D_2D_3\theta + D_3K\theta\gamma_1(1-P) + \theta\gamma_1 pq\tau + D_2\theta\gamma_1 pq,\\
B =& D_1D_2D_3(1-p) + D_2D_3\mu\theta(1-p) + D_3k\mu\theta\gamma_1(1-p) + D_3k\phi + \theta\gamma_1 + \mu pq\tau\gamma_1\\
&+ D_1D_2D_3\theta p + D_2D_3\mu p + D_2pq\mu\gamma_1 - \beta(D_2D_3\theta p\\
&+ D_2pq\theta\alpha_1\gamma_1 + D_2D_3\theta(1-p) + D_3K\theta\alpha_2\gamma_1(1-p) + pq\tau\alpha_2\gamma_1),\\
C =& D_1D_2D_3\mu(\mu+\phi)(1-R_0).
\end{aligned} \tag{24}$$

Clearly, since all the parameters are positive and $0 < p < 1$, then $A > 0$. So there are four cases to be considered depending on the sign of B and C.

Theorem 4 *The endemic equilibrium (EE) of model* (1) *has a unique positive equilibrium whenever* $R_0 > 1$.

- Case 1: If $B > 0$ and $C > 0 \iff R_0 < 1$,
  has no positive root, implying that the system has no positive equilibrium.
- Case 2: If $B < 0$ and $C < 0 \iff R_0 > 1$,
  has one positive root, which implies that the system has a unique positive equilibrium.
- Case 3: If $B > 0$ and $C < 0 \iff R_0 > 1$,
  has one positive root, which implies that the system has a unique positive equilibrium.
- Case 4: If $B < 0$ and $C > 0 \iff R_0 < 1$ and $B^2 - 4AC > 0$,
  has two positive roots, which implies that the system has two positive equilibria.

Note: Case 4 shows the possibility of the occurrence of subcritical or backward bifurcation. By backward bifurcation we mean the coexistence of a stable disease-free equilibrium with a stable endemic equilibrium when $R_0 < 1$, when bifurcation occurs, $R_0 < 1$ is only necessary but not sufficient condition for the control of the disease. So we need to show that $R_0 < 1$ is a sufficient and necessary condition for the control of the disease under consideration.

Bifurcation analysis and local stability of the endemic equilibrium

The centre manifold theorem is used to prove the existence of backward bifurcation near $R_0 = 1$, Now let $S_c = x_1$, $S_a = x_2$, $A_c = x_3$, $A_a = x_4$, $C_c = x_5$, $C_a = x_6$ such that, $N = x_1 + x_2 + x_3 + x_4 + x_5 + x_6$ so that in vector form, $X = (x_1, x_2, x_3, x_4, x_5, x_6)^T$ and the model equation can be written

in the form:

$$\frac{dX}{dt} = (f_1, f_2, f_3, f_4, f_5, f_6)^T,$$

such that,

$$\begin{aligned}
\frac{dx_1}{dt} &= f_1 = \pi p - \phi x_1 - \frac{\beta x_1(x_3 + x_4 + \alpha_1 x_5 + \alpha_2 x_6)}{N} - \mu x_1,\\
\frac{dx_2}{dt} &= f_2 = \pi(1-p) + \phi x_1 - \frac{\theta\beta x_2(x_3 + x_4 + \alpha_1 x_5 + \alpha_2 x_6)}{N} - \mu x_2,\\
\frac{dx_3}{dt} &= f_3 = \frac{\beta x_1(x_3 + x_4 + \alpha_1 x_5 + \alpha_2 x_6)}{N} - (\gamma_1 + \mu)x_3,\\
\frac{dx_4}{dt} &= f_4 = \frac{\theta\beta x_2(x_3 + x_4 + \alpha_1 x_5 + \alpha_2 x_6)}{N} - (\gamma_1 + \mu)x_4,\\
\frac{dx_5}{dt} &= f_5 = q\gamma_1 x_3 - (\gamma_2 + \tau + \mu + \delta)x_5,\\
\frac{dx_6}{dt} &= f_6 = k\gamma_1 x_4 + \tau x_5 - (\gamma_2 + \mu + \delta)x_6.
\end{aligned} \tag{25}$$

Now, the Jacobian of system (25) at the disease-free equilibrium is the same as the Jacobian of the linearized system of (1) is given as,

$$J(\epsilon^0) = \begin{bmatrix}
-\phi - \mu & 0 & -\beta K_1 & -\beta K_1 & -\beta\alpha_1 K_1 & -\beta\alpha_2 K_1\\
\phi & -\mu & -\beta\theta K_2 & -\beta\theta K_2 & -\beta\theta\alpha_1 K_2 & -\beta\theta\alpha_2 K_2\\
0 & 0 & \beta K_1 - D_1 & \beta K_1 & \beta\alpha_1 K_1 & \beta\alpha_2 K_1\\
0 & 0 & \beta\theta K_2 & \beta\theta K_2 - D_1 & \theta\alpha_1 K_2 & \theta\alpha_2 K_2\\
0 & 0 & q\gamma_1 & 0 & -D_2 & 0\\
0 & 0 & 0 & k\gamma_1 & \tau & -D_3
\end{bmatrix}, \tag{26}$$

where $K_1 = \frac{\mu p}{\phi+\mu}, K_2 = \frac{\phi+\mu(1-p)}{\phi+\mu}$. It can also be shown that the basic reproduction number by using $|J(\epsilon^0) - \lambda I| = 0$ is given as,

$$R_0 = \frac{\beta\ (\phi + \mu - \mu p)(k\theta\alpha_2 D_2\gamma_1 + \theta D_2 D_3) + \beta\mu p(\tau q\alpha_2\gamma_1 + q\alpha_1 D_3\gamma_1 + D_2 D_3)}{D_1 D_2 D_3(\phi + \mu)}.$$

Now, let $\beta = \beta^*$ be the bifurcation parameter near $R_0 = 1$ implies that,

$$\beta^* = \frac{D_1 D_2 D_3(\phi + \mu)}{(\phi + \mu - \mu p)(k\theta\alpha_2 D_2\gamma_1 + \theta D_2 D_3) + \mu p(\tau q\alpha_2\gamma_1 + q\alpha_1 D_3\gamma_1 + D_2 D_3)},$$

the linearized system of Eq. (25) has simple zero eigenvalue and all other eigenvalues are non-negative and therefore center manifold theorem can be applied to analyze the dynamics of β^*. Now, let v and w be the corresponding left and right eigenvectors associated with the simple zero eigenvalues of the Jacobian matrix of system (25) at β^* such that $vJ(\epsilon^0) = J(\epsilon^0)w = 0$, where

$v = [v_1, v_2, v_3, v_4, v_5, v_6]$ and $w = [w_1, w_2, w_3, w_4, w_5, w_6]^T$ and satisfying $v.w = 1$. Solving for

$$J(\epsilon^0)w = 0,$$
$$w_1 = \frac{-\beta^*[(D_2 + q\alpha_1\gamma_1)D_2w_3 + (D_3 + k\gamma_1)D_2w_4]}{D_2D_3(\phi + \mu)} < 0,$$
$$w_2 = \frac{D_2D_3\phi w_1 - \beta^*k_1[(D_2 + q\alpha_1\gamma_1)D_3w_3 + (D_3 + k\gamma_1)D_2w_4]}{D_2D_3} < 0,$$

$$w_3 > 0, w_4 > 0, w_5 = \frac{q\gamma_1w_3}{D_3}, w_6 = \frac{\tau\gamma_1w_3q + k\gamma_1w_4D_2}{D_2D_3} > 0,$$

and the left eigenvectors are;

$$v_1 = 0, v_2 = 0, v_3 > 0, v_4 > 0, v_5 = \frac{\beta^*(\alpha_1D_3 + \tau\alpha_2)(k_1V_3 + k_2v_4)}{D_2^2D_3},$$

and

$$v_6 = \frac{\beta^*\alpha_2(k_1V_3 + k_2V_4)}{D_3}.$$

Computation of a and b
$V_1 = V_2 = 0$, we only consider $k = 3, 4$, since, the second partial derivatives of f_5 and f_6

$$f_3 = \frac{\beta^*}{N}(x_3x_1 + x_4x_1 + \alpha_1x_5x_1 + \alpha_2x_6x_1) - D_1x_3,$$
$$f_4 = \frac{\beta^*}{N}(x_3x_2 + x_4x_2 + \alpha_1x_5x_2 + \alpha_2x_2x_6) - D_1x_4,$$
$$\frac{\partial^2 f_3}{\partial x_3\partial x_1} = \frac{\beta^*}{N} = \frac{\partial^2 f_3}{\partial x_4\partial x_1}, \frac{\partial^2 f_3}{\partial x_5\partial x_1} = \frac{\beta^*\alpha_1}{N}, \frac{\partial^2 f_3}{\partial x_6\partial x_1} = \frac{\beta^*\alpha_2}{N},$$
$$\frac{\partial^2 f_4}{\partial x_3\partial x_2} = \frac{\beta^*\theta}{N} = \frac{\partial^2 f_4}{\partial x_4\partial x_2}, \frac{\partial^2 f_4}{\partial x_5\partial x_2} = \frac{\beta^*\theta\alpha_1}{N}, \frac{\partial^2 f_4}{\partial x_6\partial x_2} = \frac{\beta^*\theta\alpha_2}{N},$$
$$a = v_3\sum_{i,j=3}^{6} w_iw_j\frac{\partial^2 f_3}{\partial x_i\partial x_j}(0,0) + v_4\sum_{i,j=3}^{6} w_iw_j\frac{\partial^2 f_4}{\partial x_i\partial x_j}(0,0),$$
$$a = \frac{\beta^*}{N^0}(w_1v_3 + \theta w_2v_4)(w_3 + w_4 + w_5 + w_6) < 0,$$
$$b = v_3\sum_{i=3}^{6} w_i\frac{\partial^2 f_3}{\partial x_i\partial\beta^*}(0,0) + v_4\sum_{i=3}^{6} w_i\frac{\partial^2 f_4}{\partial x_i\partial\beta^*}(0,0),$$
$$b = (v_3\frac{S_c^0}{N^0} + \theta v_4\frac{S_a^0}{N^0})(w_3 + w_4 + w_5 + w_6) > 0,$$

$a < 0$ and $b > 0$, thus, from the centre manifold theorem, we derive the following:

Theorem 5 *The Hepatitis-B model undergoes a backward bifurcation at $R_0 = 1$ and when $\beta^* < 0$ changes to $\beta^* > 0$, the equilibrium changes its stability from stable to unstable. Corresponding a negative unstable equilibrium becomes positive and asymptotically stable. Thus, the bifurcation that occurred is stable, and hence, $R_0 < 1$ is a necessary and sufficient condition for the Hepatitis B control.*

Global stability of the endemic equilibrium point

Theorem 6 *The endemic equilibrium (EE), ϵ^*, of model (1) is globally asymptotically stable (GAS) if $R_0 > 1$ and unstable if $R_0 < 1$.*

Proof We construct a Lyapunov function with Goh-Voltera definition as follows,

$$\begin{aligned} V = &\left(S_c - S_c^* - S_c^* ln\left(\frac{S_c}{S_c^*}\right)\right) + \left(S_a - S_a^* - S_a^* ln\left(\frac{S_a}{S_a^*}\right)\right) + \left(A_c - A_c^* - A_c^* ln\left(\frac{A_c}{A_c^*}\right)\right) \\ &+ \left(A_a - A_a^* - A_a^* ln\left(\frac{A_a}{A_a^*}\right)\right) + W_1\left(C_c - C_c^* - C_c^* ln\left(\frac{C_c}{C_c^*}\right)\right) \\ &+ W_2\left(C_a - C_a^* - C_a^* ln\left(\frac{C_a}{C_a^*}\right)\right). \end{aligned} \tag{27}$$

Taking the derivative of V with respect to t, we have

$$\begin{aligned} V' = &\left(1 - \frac{S_c^*}{S_c}\right) S_c' + \left(1 - \frac{S_a^*}{S_a}\right) S_a' + \left(1 - \frac{A_c^*}{A_c}\right) A_c' + \left(1 - \frac{A_a^*}{A_a}\right) A_a' \\ &+ W_1\left(1 - \frac{C_c^*}{C_c}\right) C_c' + W_2\left(1 - \frac{C_a^*}{C_a}\right) C_a', \end{aligned} \tag{28}$$

substituting for $S_c', S_a', A_c', A_a', C_c', C_a'$ gives,

$$\begin{aligned} V' = &\left(\pi p - \lambda S_c - \mu S_c - \frac{S_c^*}{S_c}\left(\pi p - \lambda S_c - \mu S_c\right)\right) \\ &+ \left(\pi(1-p) - \theta\lambda S_a - \mu S_a - \frac{S_a^*}{S_a}\left(\pi(1-p) - \theta\lambda S_a - \mu S_a\right)\right) \\ &+ \left(\lambda S_c - (\gamma_1 + \mu) A_c - \frac{A_c^*}{A_c}\left(\lambda S_c - (\gamma_1 + \mu) A_c\right)\right) \\ &+ \left(\theta\lambda S_a - (\gamma_1 + \mu) A_a - \frac{A_a^*}{A_a}\left(\theta\lambda S_a - (\gamma_1 + \mu) A_a\right)\right) \\ &+ \left(q\gamma_1 A_c - (\gamma_2 + \mu + \delta) C_c - \frac{C_c^*}{C_c}\left(q\gamma_1 A_c - (\gamma_2 + \mu + \delta) C_c\right)\right) \\ &+ \left(k\gamma_1 A_a - (\gamma_2 + \mu + \delta) C_a - \frac{C_a^*}{C_a}\left(k\gamma_1 A_a - (\gamma_2 + \mu + \delta) C_a\right)\right) \\ = &\left(\lambda S_c^* + \mu S_c^* - \mu S_c - \frac{S_c^{*2}}{S_c} - \lambda\mu\frac{S_c^{*2}}{S_c} + \lambda S_c^* + \mu S_c^*\right) \\ &+ \left(\theta\lambda S_a^* + \mu S_a^* - \theta\lambda S_a - \mu S_a - \theta\lambda\frac{S_a^{*2}}{S_a} - \mu\frac{S_a^{*2}}{S_a} + \theta\lambda S_a^* + \mu S_a^*\right) \\ &+ \left(\lambda S_c - (\gamma_1 + \mu) A_c - \lambda\frac{A_c^*}{A_c} S_c + (\gamma_1 + \mu) A_c^*\right) + \left(\theta\lambda S_a - (\gamma_1 + \mu) A_a - \theta\lambda\frac{A_a^*}{A_a} S_a + (\gamma_1 + \mu) A_a^*\right) \\ &+ W_1\left(q\gamma_1 A_c - (\gamma_2 + \mu + \delta) C_c - q\gamma_1\frac{C_c^*}{C_c} A_c + (\gamma_2 + \mu + \delta) C_c^*\right) \\ &+ W_2\left(k\gamma_1 A_a - (\gamma_2 + \mu + \delta) C_a - k\gamma_1\frac{C_a^*}{C_a} A_a + (\gamma_2 + \mu + \delta) C_a^*\right). \end{aligned}$$

Solving for W_1 and W_2 by equating the coefficient of A_c, A_a, C_c, C_a to zero, we have, $W_1 = \frac{\gamma_1 + \mu}{q\gamma_1}$

and $W_2 = \frac{\gamma_1+\mu}{k\gamma_1}$.

$$
\begin{aligned}
V^{'} &= 2\lambda S_c^* - \lambda\frac{S_c^{*2}}{S_c} + 2\mu S_c^* - \mu S_c - \mu\frac{S_c^{*2}}{S_c} + 2\theta\lambda S_a^* - \theta\lambda\frac{S_a^{*2}}{S_a} + 2\mu S_a^* - \mu S_a - \mu\frac{S_a^{*2}}{S_a} \\
&- \lambda\frac{A_c^*}{A_c}S_c + (\gamma_1+\mu)A_c^* - \theta\lambda\frac{A_a^*}{A_a}S_a + (\gamma_1+\mu)A_a^* - (\frac{\gamma_1+\mu}{q\gamma_1})(\gamma_2+\mu+\delta)C_c \\
&+ \left(\frac{\gamma_1+\mu}{q\gamma_1}\right)(\gamma_2+\mu+\delta)C_c^* - \left(\frac{\gamma_1+\mu}{q\gamma_1}\right)q\gamma_1\frac{C_c^*}{C_c}A_c - \left(\frac{\gamma_1+\mu}{k\gamma_1}\right)(\gamma_2+\mu+\delta)C_a \\
&+ \left(\frac{\gamma_1+\mu}{k\gamma_1}\right)(\gamma_2+\mu+\delta)C_a^* - \left(\frac{\gamma_1+\mu}{k\gamma_1}\right)k\gamma_1\frac{C_a^*}{C_a}A_a.
\end{aligned}
$$

From third and fourth equation of system (1) at the steady state, we obtain $A_c^*(\gamma_1+\mu) = \lambda S_c^*$ and $A_a^*(\gamma_1+\mu) = \theta\lambda S_a^*$, respectively, hence by simplification

$$
\begin{aligned}
V^{'} &\leq \lambda S_c^*\left(3 - \frac{S_c^*}{S_c} - \frac{A_c^* S_c}{A_c S_c^*} - \frac{C_c^* A_c}{C_c A_c^*}\right) + \theta\lambda S_a^*\left(3 - \frac{S_a^*}{S_a} - \frac{A_a^* S_a}{A_a S_a^*} - \frac{C_a^* A_a}{C_a A_a^*}\right) \\
&+ \mu S_c^*\left(2 - \frac{S_c^*}{S_c} - \frac{S_c}{S_c^*}\right) + \mu S_a^*\left(2 - \frac{S_a^*}{S_a} - \frac{S_a}{S_a^*}\right),
\end{aligned}
$$

applying the arithmetic-geometric mean relation, we have

$$\left(3 - \frac{S_c^*}{S_c} - \frac{A_c^* S_c}{A_c S_c^*} - \frac{C_c^* A_c}{C_c A_c^*}\right) \leq 0,$$

$$\left(3 - \frac{S_a^*}{S_a} - \frac{A_a^* S_a}{A_a S_a^*} - \frac{C_a^* A_a}{C_a A_a^*}\right) \leq 0,$$

and

$$\left(2 - \frac{S_c^*}{S_c} - \frac{S_c}{S_c^*}\right) \leq 0,$$

$$\left(2 - \frac{S_a^*}{S_a} - \frac{S_a}{S_a^*}\right) \leq 0.$$

Hence, $V^{'} \leqslant 0$. The strict equality condition $V^{'} = 0$ holds only at $S_c = S_c^*, A_c = A_c^*, C_c = C_c^*, S_a = S_a^*, A_a = A_a^*$ and $C_c = C_c^*$. Thus the endemic equilibrium ϵ^* is the only invariant set of the model 1. Therefore, the result follows by applying Lasalle's invariance principle [29]. Hence the endemic equilibrium (EE) ϵ^* of the model (1) is globally asymptotically stable (GAS). ■

Following Figure 2, Figure 3, Figure 4, and Figure 5 verify the analytical result of the global stability of endemic equilibrium. The plots show that any change in the number of acutely or chronically infected individuals provided the basic reproduction number is greater than unity, the endemic equilibrium will return to its equilibrium points. Biologically this statement means that, despite the small or big changes in the number of acute or chronic infected individuals Hepatitis B will persist if the basic reproduction number is greater than one.

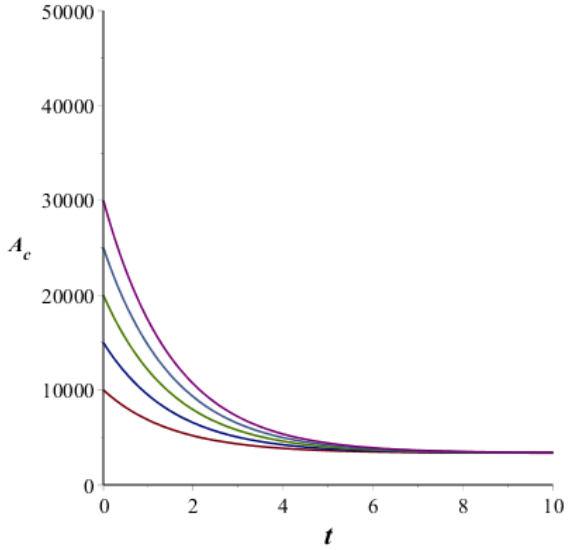

Figure 2. Time series plot of the HBV infection model for acutely infected children utilizing different initial conditions with the parameter values in Table 1.

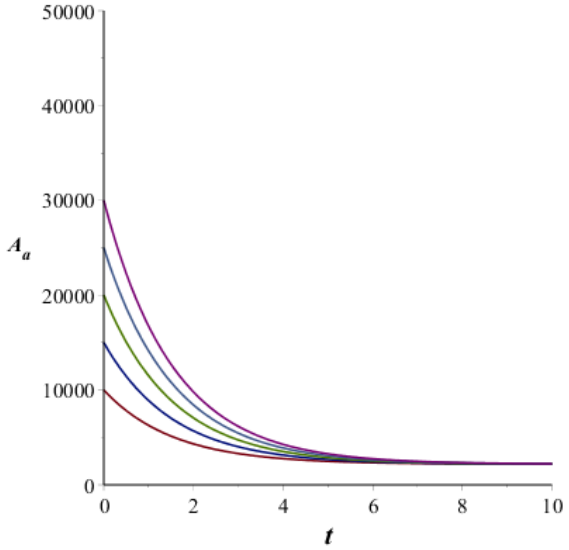

Figure 3. Time series plot of the HBV infection model for acutely infected adults utilizing different initial conditions with the parameter values in Table 1.

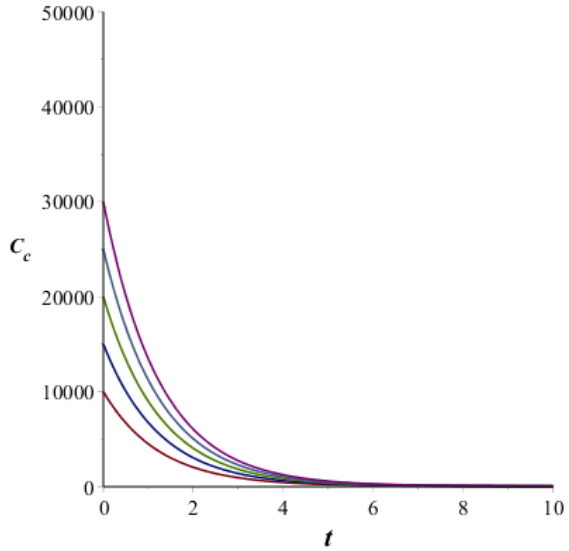

Figure 4. Time series plot of the HBV infection model for chronically infected children utilizing different initial conditions with the parameter values in Table 1.

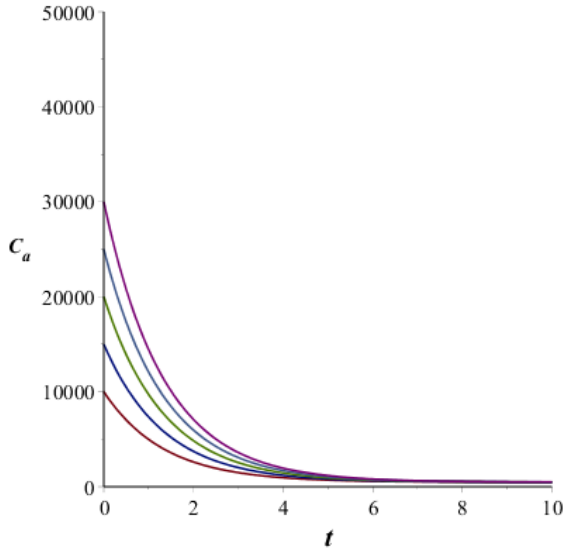

Figure 5. Time series plot of the HBV infection model for chronically infected adults utilizing different initial conditions with the parameter values in Table 1.

4 Model fitting and parameter estimation

This section contains detailed information on the proposed model's validation while using the actual Hepatitis B Viral (HBV) cases obtained from [6] for the Free State, South Africa from 2015 to 2019. Having actual cases for a disease seems to have several benefits including the model's validation and optimizing the values of some biological parameters unknown at the beginning of the analysis. Among several available tools for finding unknown parameters of an epidemic

model, we have employed the method of nonlinear least-squares curve fitting. As shown by Figure 6, the method has fitted the real HBV cases with very small errors that are also confirmed by the residue plot shown in Figure 7. Figure 8 for the BoxWhisker plot shows the reasonable agreement between actual HBV cases and those obtained from the simulations for A_c class of the proposed model.

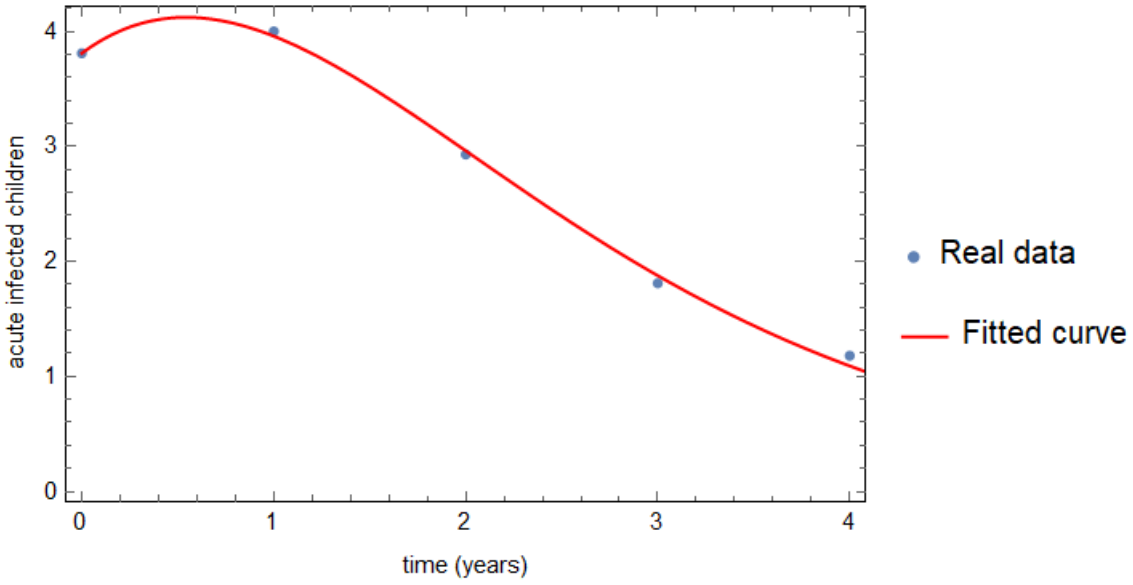

Figure 6. The best curve fitting for the real cases of the acutely infected children from the proposed model given in system (1).

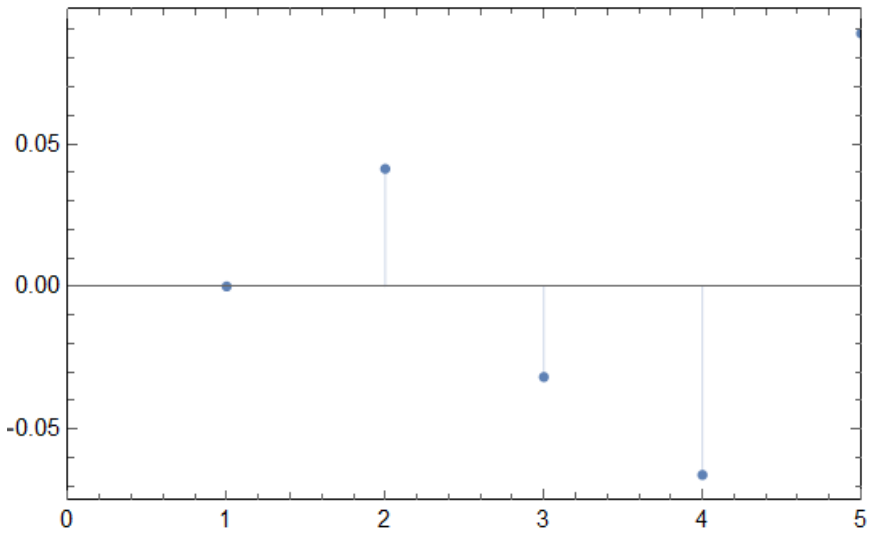

Figure 7. The residuals plot for the difference between the real cases of the acutely infected children and simulations of the proposed model given in system (1).

Regarding the real and the predicted cases of HBV, the standard error and their respective confidence intervals are computed in Table 2 wherein the standard error for each value is found to be as minimum as 10^{-2} with 95% confidence interval.

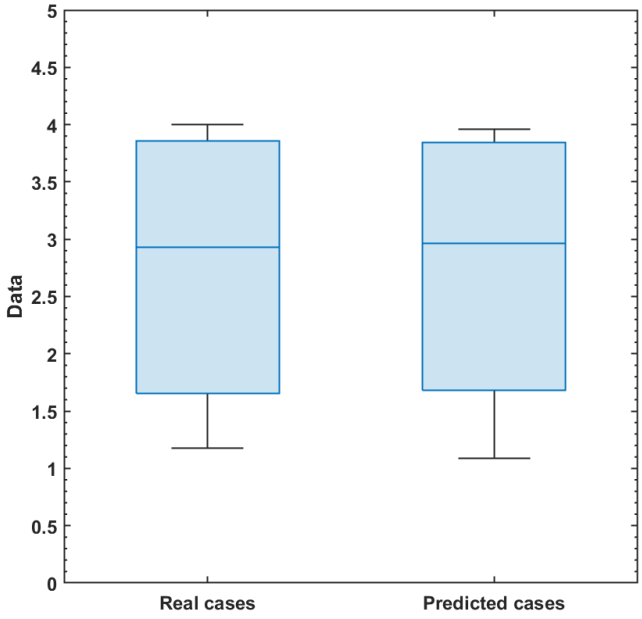

Figure 8. The BoxWhisker plot for the real cases of the acute infected children and simulations of the proposed model given in system (1).

Table 2. Comparison between the number of real acute infected children and predicted ones with associated standard errors and the confidence intervals.

Observed	Predicted	Standard Error	Confidence Interval
3.81	3.81	0.0611803	{3.64014, 3.97986}
4.00	3.95873	0.0729167	{3.75628, 4.16118}
2.93	2.9618	0.0719738	{2.76197, 3.16163}
1.81	1.87615	0.065646	{1.69389, 2.05841}
1.18	1.09122	0.0625195	{0.917637, 1.2648}

The seven-point summary statistics included in Table 3 show that the predicted values from the model (1) have reasonably acceptable results containing minimum, first quartile, median, mean, third quartile, maximum, and standard error.

Table 3. Summary statistics for the real data, and the predicted data points obtained under simulations of the model (1) for the acutely infected children A_c.

Data	Min.	1st Qu.	Median	Mean	3rd Qu.	Max.	SD
Actual cases	1.18	1.65	2.93	2.75	3.86	4.00	1.23
Predicted cases	1.09	1.68	2.96	2.74	3.85	3.96	1.24

The fitted parameters including π, β, γ_1, and γ_2 are tabulated in Table 4 wherein we have obtained these values with very small standard error with p-value < 0.05 under 95% confidence interval. For example, the contact rate (β) has fitted value equal to 9.3471×10^{-1} with standard error of 1.67859×10^{-2} and p-value of 6.22714×10^{-7}. Using the values given in this table, the approximate value for the basic reproductive number is obtained as 1.15945 which presents the reality of the scenario under the present analysis regarding the persistence of the HBV.

Table 4. Baseline values and ranges for parameters of model (1).

Parameter	Baseline (Range)	Units	Sources
μ	0.6384 (0.425, 0.745)	year^{-1}	Estimated by [24]
π	3.30 (2.39, 4.74)	year^{-1}	Fitted
p	0.02 (0.001, 0.057)	year^{-1}	Estimated by [24]
ϕ	0.2 (0.15, 0.38)	year^{-1}	Estimated by [24]
β	$9.3471 \times 10^{-1}(8.88105 \times 10^{-1}, 9.81316 \times 10^{-1})$	year^{-1}	Fitted
q	0.71 (0.59, 0.87)	year^{-1}	Estimated by [16]
θ	0.8020 (0.325, 0.850)	year^{-1}	Fitted
k	0.31 (0.23, 0.47)	year^{-1}	Estimated by [16]
α_1, α_2	0.043, 0.004 (0.0023, 0.0678)	year^{-1}	Estimated by [16]
γ_1	0.009 (0.0004, 0.02)	year^{-1}	Fitted
γ_2	0.03 (0.015, 0.054)	year^{-1}	Fitted
δ	0.08 (0.052, 0.089)	year^{-1}	Estimated by [24]
τ	0.056 (0.043, 0.068)	year^{-1}	Estimated by [24]

5 Sensitivity analysis

In this subsection, we analyze the proposed HVB model using the forward sensitivity index in relation to the reproduction number R_0 with respect to the biological parameters of the model. This method is used to determine the most sensitive parameters of the model and those parameters with positive signs are regarded as the most sensitive for increasing the value of R_0 while parameters with negative signs are sensitive to the decrease of R_0 [30, 31].

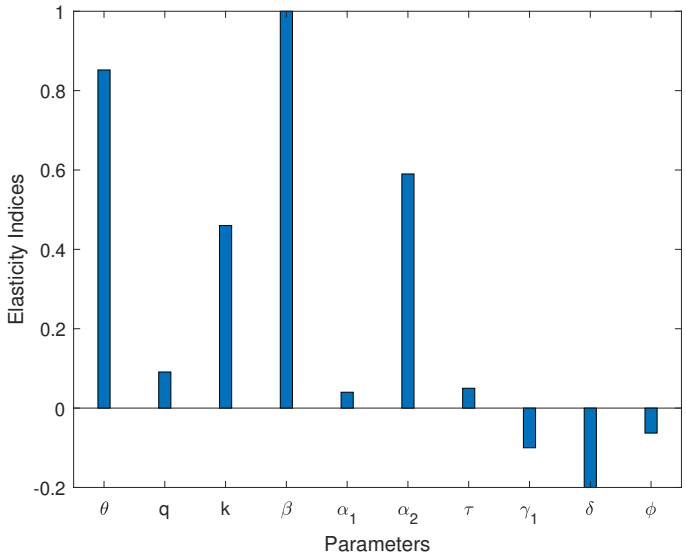

Figure 9. Elasticity indices versus the parameters.

The optimization of the result is obtained by determining the sensitivity status of each parameter and their impacts on the control of the spread of HBV infections in the population [27, 32]. We denote by $\chi_\theta^{R_0}$ the normalized local sensitivity index of the R_0 with respect to the θ, and is given by

$$\chi_\theta^{R_0} = \frac{\theta}{R_0} \times \frac{\partial R_0}{\partial \theta}. \tag{29}$$

We get the indices below for the R_0 with respect to parameters shown in Table 4. The results given in the forward normalized sensitivity indices Table 5 with a Bar chart pictorial representation revealed that the top and most sensitive epidemiological parameters to effectively contain the spread of the HBV viral infection in order of preference are: (i) β followed by (ii) θ, respectively. Recall that the parameter θ is a modification parameter reducing the susceptibility of adult individuals and therefore it goes with the immune system of the person, so without loss of generality, we assumed θ to be constant. The parameter β is therefore prioritized in order to control the spread of HBV viral infection in South Africa.

Table 5. Forward normalized sensitivity indices.

Parameter	Elasticity Indices	Values of the Elasticity index
θ	$\chi_{\theta}^{R_0}$	0.8521
q	$\chi_{q}^{R_0}$	0.0910
k	$\chi_{k}^{R_0}$	0.4600
β	$\chi_{\beta}^{R_0}$	1.0000
α_1	$\chi_{\alpha_1}^{R_0}$	0.0400
α_2	$\chi_{\alpha_2}^{R_0}$	0.5900
τ	$\chi_{\tau}^{R_0}$	0.0500
γ_1	$\chi_{\gamma_1}^{R_0}$	-0.1000
δ	$\chi_{\delta}^{R_0}$	-0.2000
ϕ	$\chi_{\phi}^{R_0}$	-0.0630

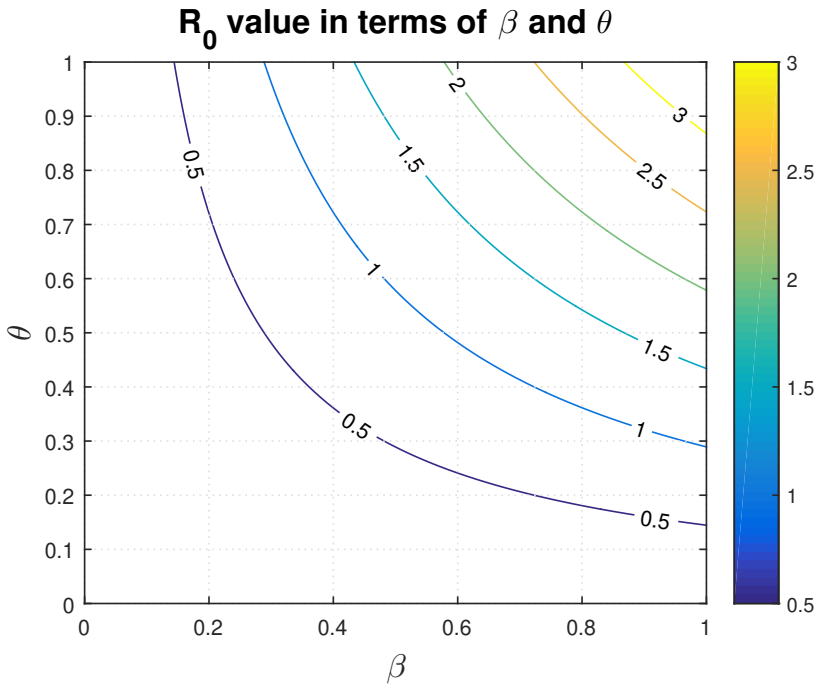

(a)

Figure 10. Cont...

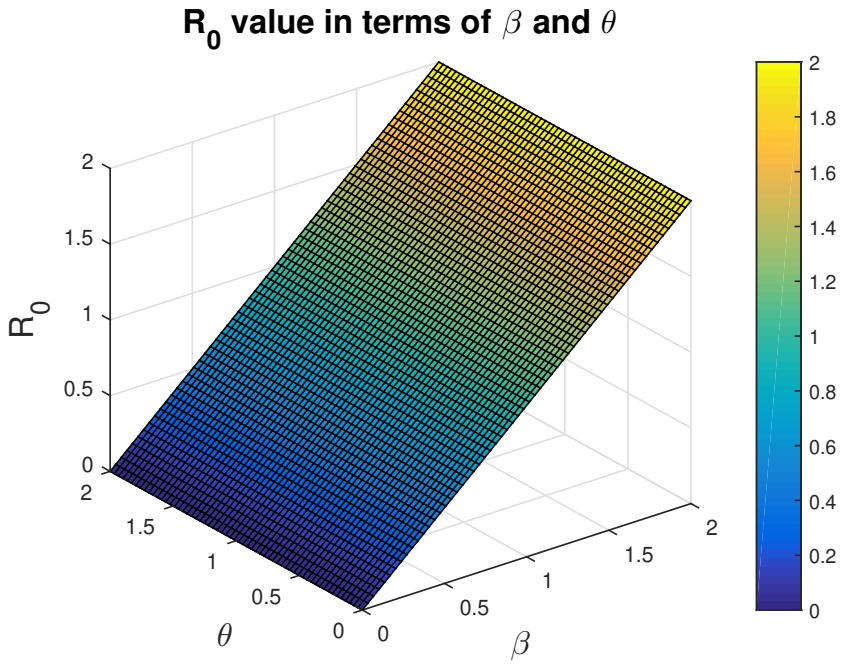

(b)

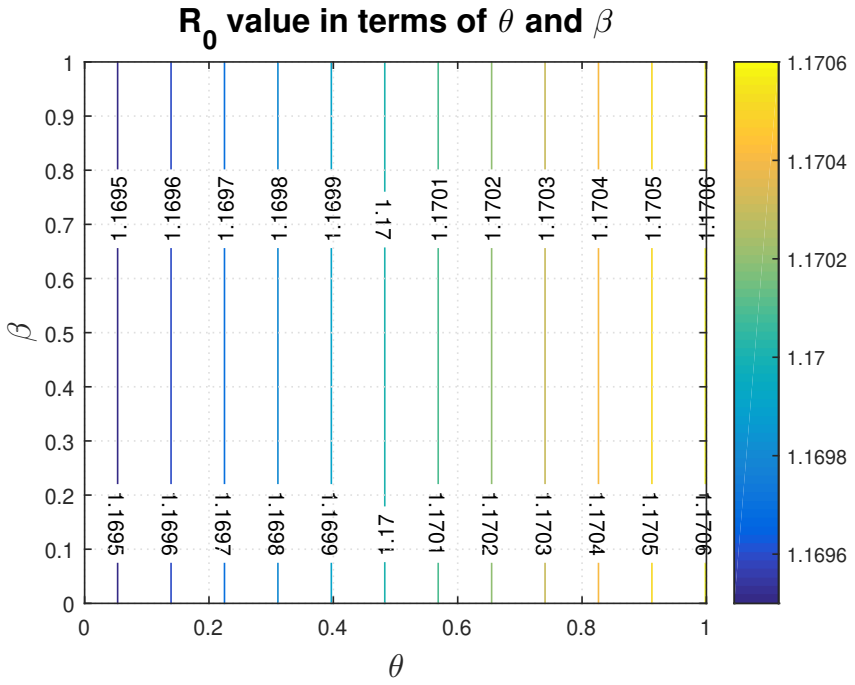

(c)

Figure 10. Cont...

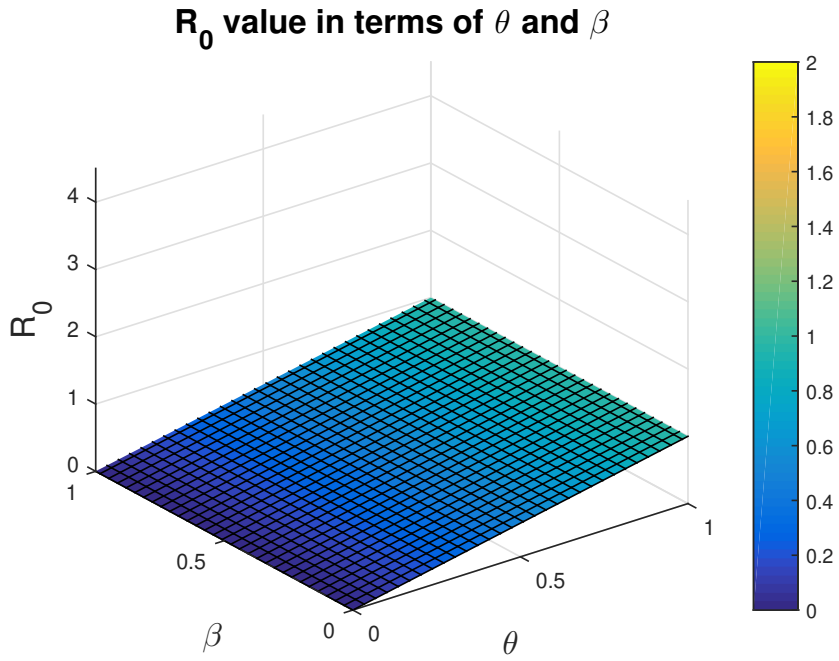

(d)

Figure 10. Contour and mesh plots of the basic reproduction number R_0 in terms of modification parameter decreasing the susceptibility of an adult θ and contact rate β as a response function.

6 Numerical simulations

This is the vantage point from which we may gain a comprehensive understanding of the model's behavior. The transmission dynamics of the governing model may be effectively explored using numerical simulations with the aid of state variables of interest. We used numerical simulations in this part to better understand the behavior of the model under investigation. We use the parameters generated by the nonlinear minimum-squares fitting technique in the immediate section to see different types of time series graphs.

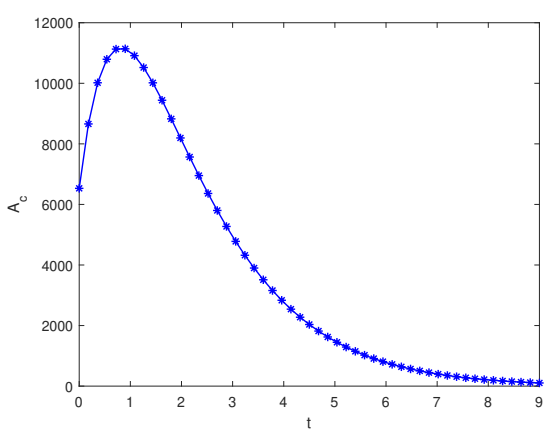

(a)

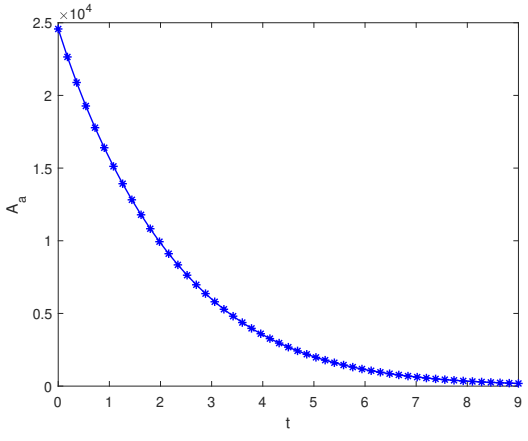

(b)

Figure 11. (a) Behavior of the state variables acutely infected children A_c, (b) acutely infected adult A_a.

Figure 11(a) and Figure 11(b) describe the behavior of acutely infected children and adults, respectively. The graph raises due to susceptible children and adults becoming infected after contracting the disease. It decreases due to the recovery and progression of acutely infected individuals into chronic compartments.

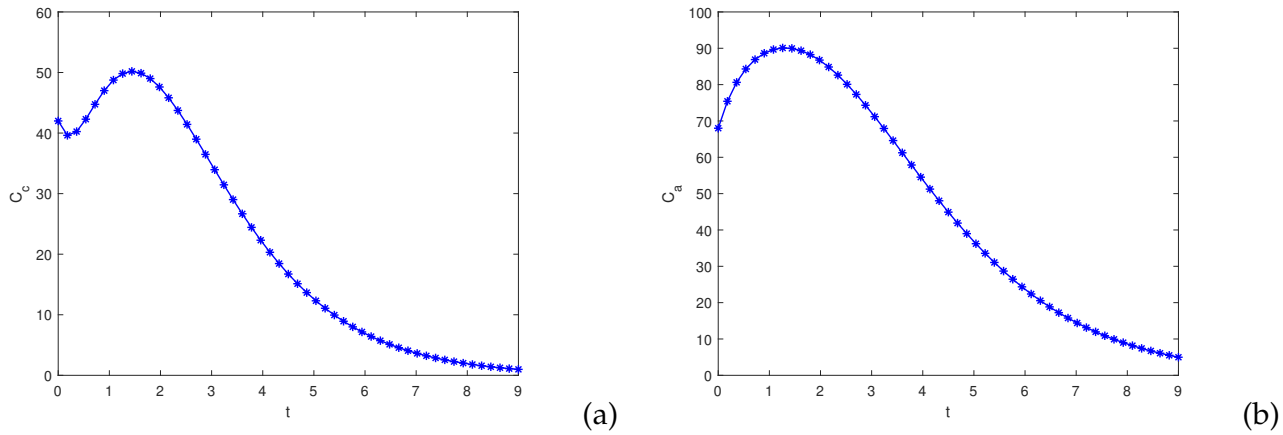

Figure 12. (a) Behavior of the state variables chronically infected children C_c, (b) chronically infected adult C_a.

Figure 12(a) and Figure 12(b) describe the behavior of chronically infected children and adults, respectively. The graph raises due to acutely infected children and adults developing chronic infection. It decreases due to the recovery of infected individuals and death due to chronic Hepatitis B.

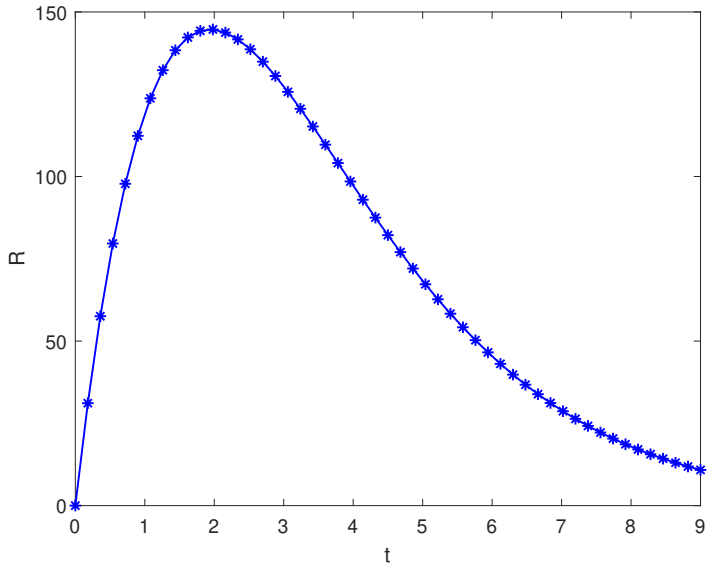

Figure 13. Behavior of the recovered individuals R.

Figure 13 describes the behavior of the recovered compartment. The graph raises due to the recovery of acutely and chronically infected individuals. It decreases due to natural death.

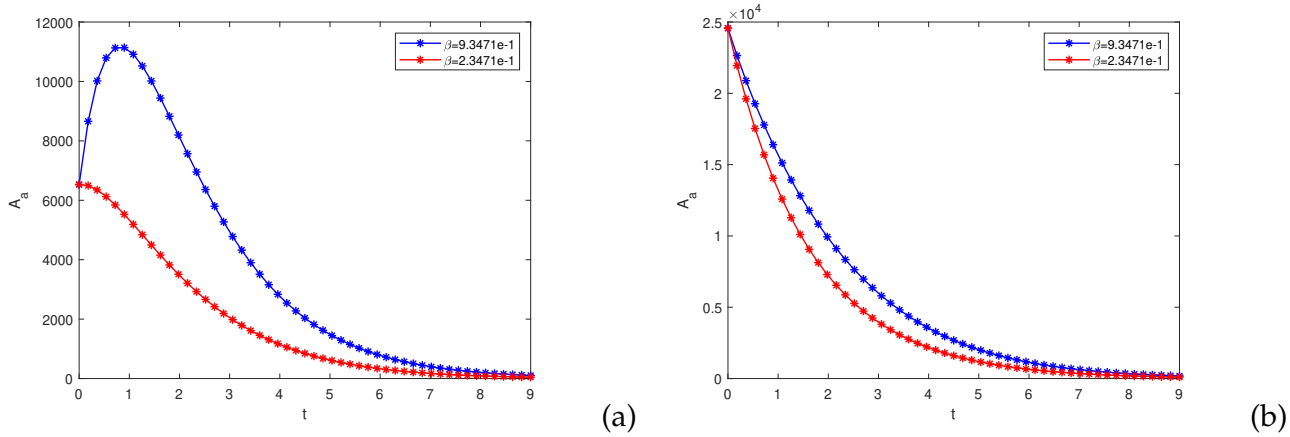

Figure 14. (a) Patterns of A_c and (b) A_a with different values of contact rate β.

Figure 14(a) and Figure 14(b) describe the behavior of acutely infected children and adults, respectively, with different values of contact rate β. The graph raises when the contact rate is greater. The more the contact rate, the more the number of acutely infected individuals.

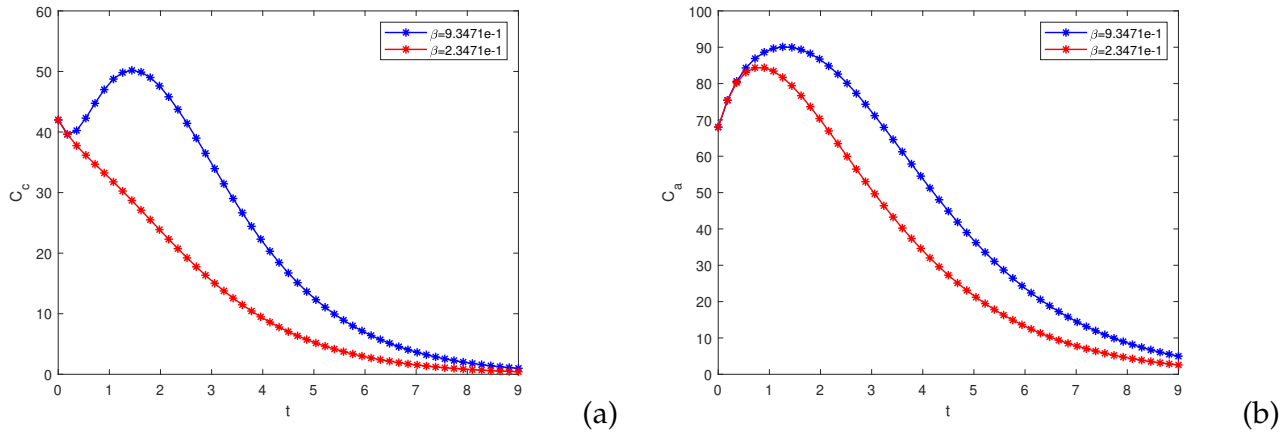

Figure 15. (a) patterns of C_c and (b) C_a with different values of contact rate β.

Figure 15(a) and Figure 15(b) describe the behavior of chronically infected children and adults, respectively, with different values of contact rate β. The graph raises when the contact rate is greater. The more the contact rate, the more the number of chronically infected individuals. Figure 16(a) and Figure 16(b) describe the behavior of acutely infected children and adults, respectively, with different values of progression rate τ from chronically infected children into adult compartments. The graph raises in the case of chronically infected adults when the rate τ is larger, and falls when the rate τ is smaller in the case of chronically infected children. The more the progression rate, the more the number of chronically infected adults and the smaller the number of chronically infected adults.

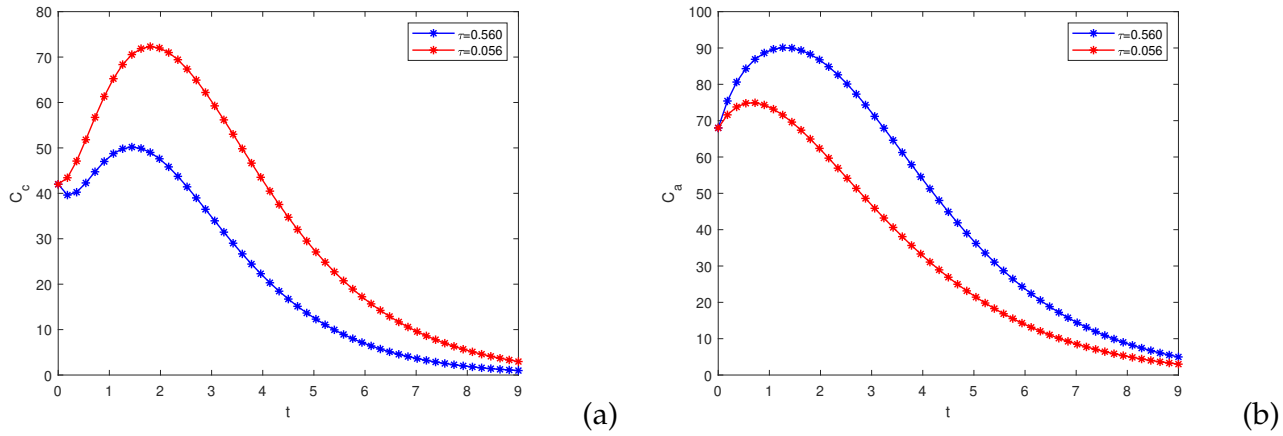

Figure 16. (a) Patterns of C_c with different values of progression rate of chronically infected children that grow into adult τ, (b) Patterns of C_a with different values of progression rate of chronically infected children that grow into adult.

7 Discussion and conclusion

An age-structured deterministic model consisting of a system of ordinary differential equations is designed to study the transmission dynamics of Hepatitis B. The analysis of the model shows that it undergoes backward bifurcation, a phenomenon in which a stable disease-free equilibrium coexists with stable endemic equilibrium (EE) when the basic reproduction number is less than one (i.e. $R_0 < 1$). The bifurcation analysis performed shows that the endemic equilibrium is locally asymptotically stable. Further analysis shows that the disease-free equilibrium is globally asymptotically stable when $R_0 < 1$ and unstable when $R_0 > 1$ while the endemic equilibrium is globally asymptotically stable when $R_0 > 1$ and unstable when $R_0 < 1$. We have estimated the model parameters using the nonlinear least-squares curve fitting method having a very minimum standard error with p-value < 0.05 under 95% confidence interval with the help of real data from South Africa. The data is extracted from [6]. The global stability of the endemic equilibrium is verified numerically in Figure 2 to Figure 5 using the fitted parameters. The graphs show the persistence of the disease with $R_0 = 1.15945$ using the parameter values in Table 4. The forward normalized sensitivity index technique is employed for sensitivity analysis. We obtained the most sensitive parameters that are essential for the control of the spread of Hepatitis B infection as summarized in Table 5 where the contact rate β has the highest elasticity index value of 1.0. Finally, we obtained some numerical simulation results describing the pattern of movement from one compartment to another. Figure 11 described the pattern of A_c and A_a, Figure 12 described the pattern of C_c and C_a and Figure 13 described the pattern of the recovered compartment. The simulation has also shown the effect of the most sensitive parameters on the model as described in Figure 14, Figure 15, and Figure 16. Figure 14 and Figure 15 show that the disease transmission decreases as the contact rate β decreases. Figure 16 shows that as the progression rate of chronic children into chronic adult τ decreases, the number of chronically infected children will increase while that of chronic adults will decrease. We suggested that to eradicate Hepatitis B in South Africa, there is a need to minimize the contact between the infected individuals and susceptible ones apart from their current control strategy of routine immunization. Acutely infected individuals should be guided on care to avoid their progression into chronically infected individuals. Treatment of chronically infected individuals should be emphasized to avoid the growth of chronically infected children into adults with the disease.

Declarations

Ethical approval

The authors state that this research complies with ethical standards. This research does not involve either human participants or animals.

Consent for publication

Not applicable

Conflicts of interest

The authors declare that they have no known competing interests regarding the work reported in this article.

Funding

Not applicable

Author's contributions

U.T.M.: Conceptualisation, Analysis, Methodology, Supervision, Writing-Original draft. Y.U.A.: Software, Numerical simulation, Investigation, Visualization, Writing-Original draft. A.Y.: Numerical simulation, Resources, Validations. S.Q.: Writing-Reviewing and Editing, Validation. S.S.M.: Conceptualisation, Methodology, Supervision. All authors documented the results, prepared the manuscript, and worked on enhancing writing quality. All authors read the final version of the manuscript and approved the results.

Acknowledgements

Not applicable

References

[1] World Health Organization (2017). *Global hepatitis report 2017*. World Health Organization. Accessed Date: July 2023.

[2] World Health Organization (2021). https://www.who.int/news-room/fact-sheets/detail/hepatitis-b. Accessed Date: July 2023.

[3] U.S. Department of Health and Human Service (2013). *Centre for Disease Control and Prevention*. https://www.cdc.gov/knowhepatitisB. Accessed Date: July 2023.

[4] Khaleel, H.A. Hepatitis B virus: can it be a vector-borne transmitted infection? *Tropical Medicine & Surgery*, 3(2), 1000186, (2015). [CrossRef]

[5] Burnett, R.J., Kramvis, A., Dochez, C. and Meheus, A. An update after 16 years of Hepatitis B vaccination in South Africa. *Vaccine*, 30, C45-C51, (2012). [CrossRef]

[6] Moonsamy, S., Suchard, M., Pillay, P. and Prabdial-Sing, N. Prevalence and incidence rates of laboratory-confirmed Hepatitis B infection in South Africa, 2015 to 2019. *BMC Public Health*, 22, 29, (2022). [CrossRef]

[7] Blackwood, J.C. and Childs, L.M. An introduction to compartmental modeling for the budding infectious disease modular. *Letters in Biomathematics*, 5(1), 195-221, (2018). [CrossRef]

[8] Bacaër, N. McKendrick and Kermack on epidemic modelling (1926–1927). In *A Short History of Mathematical Population Dynamics* (pp. 89-96). London, UK: Springer, (2011). [CrossRef]

[9] Eskandari, Z., Khoshsiar Ghaziani, R. and Avazzadeh, Z. Bifurcations of a discrete-time SIR epidemic model with logistic growth of the susceptible individuals. *International Journal of Biomathematics,* 16(06), 2250120, (2023). [CrossRef]

[10] Naik, P.A., Eskandari, Z., Shahkari, H.E. and Owolabi, K.M. Bifurcation analysis of a discrete-time prey-predator model. *Bulletin of Biomathematics,* 1(2), 111-123, (2023). [CrossRef]

[11] Li, B. and Eskandari, Z. Dynamical analysis of a discrete-time SIR epidemic model. *Journal of the Franklin Institute*, 360(12), 7989-8007, (2023). [CrossRef]

[12] Fatima, B., Yavuz, M., ur Rahman, M. and Al-Duais, F.S. Modeling the epidemic trend of middle eastern respiratory syndrome coronavirus with optimal control. *Mathematical Biosciences and Engineering*, 20(7), 11847-11874, (2023). [CrossRef]

[13] Fatima, B., Yavuz, M., ur Rahman, M., Althobaiti, A. and Althobaiti, S. Predictive modeling and control strategies for the transmission of Middle East respiratory syndrome coronavirus. *Mathematical and Computational Applications*, 28(5), 98, (2023). [CrossRef]

[14] Rahman, M.U., Alhawael, G. and Karaca, Y. Compartmental analysis of Middle Eastern respiratory syndrome coronavirus model under fractional operator with Next-Generation Matrix methods. *Fractals*, 31(10), 2340093, (2023). [CrossRef]

[15] Odionyenma, U.B., Ikenna, N. and Bolaji, B. Analysis of a model to control the co-dynamics of Chlamydia and Gonorrhea using Caputo fractional derivative. *Mathematical Modelling and Numerical Simulation with Applications,* 3(2), 111-140, (2023). [CrossRef]

[16] Liang, P., Zu, J. and Zhuang, G. A literature review of mathematical models of Hepatitis B virus transmission applied to immunization strategies from 1994 to 2015. *Journal of Epidemiology,* 28(5), 221-229, (2017). [CrossRef]

[17] Edmunds, W.J., Medley, G.F. and Nokes, D.J. The transmission dynamics and control of Hepatitis B virus in The Gambia. *Statistics in Medicine,* 15(20), 2215-2233, (1996). [CrossRef]

[18] Kretzshmer, M., Mangen, M.J., Van de Laar, M. and de Wit, A. Model based analysis of Hepatitis B vaccination strategies in Netherlands. *Vaccine,* 27(8), 1254-1260, (2009). [CrossRef]

[19] Din, A. and Abidin, M.Z. Analysis of fractional-order vaccinated Hepatitis-B epidemic model with Mittag-Leffler kernels. *Mathematical Modelling and Numerical Simulation with Applications*, 2(2), 59-72, (2022). [CrossRef]

[20] Mann, J. and Roberts, M. Modeling the epidemiology of Hepatitis B in New Zealand. *Journal of Theoretical Biology,* 269(1), 266-272, (2011). [CrossRef]

[21] Thornley, S., Bullen, C. and Roberts, M. Hepatitis in a high prevalence New Zealand population: a mathematical model applied to infection control policy. *Journal of Theoretical Biology,* 254(3), 599-603, (2008). [CrossRef]

[22] Williams, J.R., Nokes, D.J., Medley, G.F. and Anderson, R.M. The transmission dynamics of Hepatitis B in the UK: a mathematical model for evaluating cost and effectiveness of immunization programs. *Epidemiology & Infection,* 116(1), 71-89, (1996). [CrossRef]

[23] Zhao, S., Xu, Z. and Lu, Y. A mathematical model of Hepatitis B virus transmission and its application for vaccination strategy in China. *International Journal of Epidemiology,* 29(4), 744-752, (2000). [CrossRef]

[24] Abdulrahman, S., Tech, M., Akinwande, N.I., Awojoyogbe, O.B. and Abubakar, U.Y. Mathematical analysis of the control of Hepatitis B virus in a population with vital dynamics. *The Pacific Journal of Science and Technology,* 14(1), 188-204, (2013).

[25] Van den Driessche, P. and Wanmough, J. Reproduction numbers and sub-threshold endemic equilibria for compartimental models of disease transmition. *Mathematical Biosciences*, 180(1-2), 29-48, (2002). [CrossRef]

[26] DeJesus, E.X. and Kaufman, C. Routh-Hurwitz criterion in the examination of eigenvalues of a system of nonlinear ordinary differential equations. *Physical Review A*, 35(12), 5288, (1987). [CrossRef]

[27] Mustapha, U.T., Qureshi, S., Yusuf, A. and Hincal, E. Fractional modeling for the spread of Hookworm infection under Caputo operator. *Chaos, Solitons & Fractals*, 137, 109878, (2020). [CrossRef]

[28] Castillo-Charez, C. and Song, B. Dynamical model of tuberculosis and their applications. *Mathematical Biosciences and Engineering*, 1(2), 361-404, (2004). [CrossRef]

[29] La Salle, J.P. *The stability of dynamical systems*. Regional conference series in applied mathematics. SIAM: Philadelphia, (1976).

[30] Mustapha, U.T. and Hincal, E. An optimal control of hookworm transmissions model with differential infectivity. *Physica A: Statistical Mechanics and its Applications*, 545, 123625, (2020). [CrossRef]

[31] Yusuf, A., Mustapha, U.T., Sulaiman, T.A., Hincal, E. and Bayram, M. Modeling the effect of horizontal and vertical transmissions of HIV infection with Caputo fractional derivative. *Chaos, Solitons & Fractals*, 145, 110794, (2021). [CrossRef]

[32] Usaini, S., Mustapha, U.T. and Sabiu, S.M. Modelling scholastic underachievement as a contagious disease. *Mathematical Methods in the Applied Sciences*, 41(18), 8603-8612, (2018). [CrossRef]

Bulletin of Biomathematics (BBM)
(https://bulletinbiomath.org)

How to cite this article: Mustapha, U.T., Ahmad, Y.U., Yusuf, A., Qureshi, S. & Musa, S.S. (2023). Transmission dynamics of an age-structured Hepatitis-B infection with differential infectivity. *Bulletin of Biomathematics*, 1(2), 124-152. https://doi.org/10.59292/bulletinbiomath.2023007